Separation and Purification Technology 355 (2025) 129635

Contents lists available at ScienceDirect

Separation and Purification Technology

journal homepage: www.elsevier.com/locate/seppur

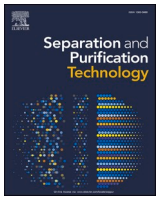

Periodic membrane fractionation of freshwater organic matter reveals various reactivity patterns during chlorine/chloramine disinfection

Karlien Dejaeger [a,b,c], Marjolein Vanoppen [a,d], Justine Criquet [b,e], Gabriel Billon [b], Cécile Vignal [c], Emile R. Cornelissen [a,d,f,*]

[a] PaInT, Particle and Interfacial Technology Group, Department of Green Chemistry and Technology, Faculty of Bioscience Engineering, Ghent University, Coupure Links 653 9000, Ghent, Belgium
[b] Univ. Lille, CNRS, UMR 8516 - LASIRE, Laboratoire de Spectroscopie pour les Interactions, la Réactivité et l'Environnement, F-59000, Lille, France
[c] Univ. Lille, Inserm, CHU Lille, U1286 - INFINITE - Institute for Translational Research in Inflammation F-59000, Lille, France
[d] Centre for Advanced Process Technology for Urban Resource Recovery (CAPTURE), Frieda Saeysstraat 1 9052, Ghent, Belgium
[e] Institut Universitaire de France (IUF), France
[f] KWR Water Research Institute, Groningenhaven 7 3433 PE, Nieuwegein, the Netherlands

ARTICLE INFO

Editor: V Tarabara

Keywords:
Disinfection by-products
Drinking water
Ultrafiltration
Nanofiltration

ABSTRACT

Although drinking water disinfection has significantly reduced mortality from waterborne diseases, the formation of potentially harmful disinfection by-products (DBPs) remains a concern today. These DBPs emerge from the reaction of dissolved organic matter (DOM) with chlor(am)ine during disinfection. Identifying these DBP precursors from heterogeneous and complex DOM mixtures is challenging and to address this, a novel membrane fractionation protocol was developed to isolate and identify the organic DBP precursors from fresh water sources. A tight ultrafiltration and nanofiltration membrane were carefully selected to partition DOM into three molecular weight (MW) fractions: high (>20 kDa), medium (0.3–20 kDa) and low (<0.3 kDa) as defined by high performance-size exclusion chromatography- total organic carbon analysis. A mathematical tool was developed to optimize the fractionation protocol. Therefore, ultrafiltration was executed before nanofiltration and the concentration factor was maximized without inducing fouling to obtain the purest fractions. The mathematical tool was also set in place to predict the necessary diafiltration factor for each individual fractionation experiment based on the initial organic matter composition of the surface water allowing the fractionation protocol to be effective at all times. The protocol was applied to surface water samples collected six times across three seasons yielding a fraction enriched in high MW compounds (up to 50 %), a fraction having more than 80 % of medium MW compounds and a fraction only containing low MW compounds. Although the medium MW fraction showed the highest reactivity for the majority of the investigated DBPs, the low MW fraction showed high reactivity for iodinated trihalomethanes during chlorination and for haloacetonitriles during chloramination. The high MW fraction had the lowest reactivity towards DBPs, which can have important implications for a drinking water treatment since this fraction is generally the most effectively removed by *e.g.* coagulation, while the more important fractions for DBP formation such as the medium and low MW compounds remain in the water until the disinfection step.

Abbreviations: CF, concentration factor; DF, diafiltration factor; DBP, disinfection by-product; DOC, dissolved organic carbon; DOM, dissolved organic matter; HAM, haloacetamide; HAA, haloacetic acid; HAN, haloacetonitrile; HMW, high molecular weight; HPSEC-TOC, high performance size exclusion chromatography – total organic carbon detection; LC-OCD, liquid chromatography- organic carbon detection, LMW, low molecular weight; MMW, medium molecular weight; MF, microfiltration; MW, molecular weight; MWCO, molecular weight cut-off; NF, nanofiltration; PEG, polyethylene glycol; (S)UV(A)$_{254}$, (specific) ultraviolet absorption at 254 nm; TMP, transmembrane pressure; THM, trihalomethane; UF, ultrafiltration.

* Corresponding author at: Coupure Links 653 9000, Ghent, Belgium.
E-mail addresses: karlien.dejaeger@ugent.be, karlien.dejaeger@univ-lille.fr (K. Dejaeger), marjolein.vanoppen@ugent.be (M. Vanoppen), justine.criquet@univ-lille.fr (J. Criquet), gabriel.billon@univ-lille.fr (G. Billon), cecile.vignal2@univ-lille.fr (C. Vignal), emile.cornelissen@ugent.be, emile.cornelissen@kwrwater.nl (E.R. Cornelissen).

https://doi.org/10.1016/j.seppur.2024.129635
Received 17 June 2024; Received in revised form 23 August 2024; Accepted 9 September 2024
Available online 10 September 2024

1. Introduction

Drinking water disinfection with chlorine has been one of the most impactful inventions of the 20th century due to its ability to inactivate waterborne pathogens [1]. However, dissolved organic matter (DOM) present in drinking water resources results in the formation of disinfection by-products (DBPs) by interaction with chlorine and other disinfectants. These DBPs are associated with negative health issues such as bladder and colorectal cancer [2,3]. While over 700 organic DBPs have been analytically identified in drinking water, only four trihalomethanes (THMs) and five haloacetic acids (HAAs) formed during chlorination processes are currently regulated in Europe [4,5]. Remarkably, many other DBPs, such as the nitrogenous haloacetamides (HAM) or haloacetonitriles (HAN) remain unregulated due to their lower occurrence in drinking water, despite their higher toxicity potential [6]. In addition, iodinated compounds emerge in the presence of iodide in the water, and their toxicity within a class of DBPs surpasses that of chlorinated and brominated analogs [6,7].

Characterizing the organic precursors of these DBPs and removing them from the drinking water before disinfection is crucial. However, DOM is a complex and heterogenous mixture of compounds complicating the search for DBP precursors [8]. To characterize DOM and to link its properties to the formation of different DBP families, DOM is fractionated into groups with similar physical or chemical characteristics using membrane or resin fractionation [9,10]. Hydrophobic moieties are mainly responsible for the formation of regulated by-products, while hydrophilic compounds often form more unregulated DBPs. This can vary based on factors such as the specific ultraviolet absorption at 254 nm ($SUVA_{254}$) of the raw water or on experimental procedures used, such as the column capacity factor during resin fractionation [11]. Furthermore, resin fractionation requires acidification of the water samples which might change the chemical and physical properties of the DOM and affect their reactivity [12]. Membrane fractionation seems to be a preferable alternative as it avoids acidification or other sample preparation. The fractionation is typically performed using a series of dead-end, stirred cell ultrafiltration (UF) steps with decreasing molecular weight cut-off (MWCO) values [11]. The defined molecular weight (MW)-range of each fraction is based on the MWCO of the UF membranes used. For example, compounds passing a 50 kDa membrane, but retained by a subsequent 10 kDa membrane, are categorized as the 10–50 kDa fraction [13–15]. However, only few studies characterized the fractions afterwards using high performance size exclusion chromatography (HPSEC) or field flow fractionation. These studies showed that the fractions obtained from membrane fractionation have largely overlapping MW-ranges and that the actual MW-range of the fractions is much lower than defined by the MWCO. For example, the 10–30 kDa fraction actually contained DOM in the range of 0.89 to 3.34 kDa [13–15]. Therefore, no clear correlations nor conclusive trends were found between the different obtained membrane fractions and DBP formation after disinfection [11].

A discontinuous cross-flow membrane fractionation was recently developed to investigate the fouling potential of organic matter fractions obtained from seawater [16]. Fractionation was executed using one nanofiltration (NF) and one UF membrane, with diafiltration added in each step to increase the purification of the different fractions. The aim of the membrane fractionation was to separate the DOM in three fractions; biopolymers, humic substances + building blocks and low molecular weight (LMW) compounds. These fractions were collected and analyzed using liquid chromatography – organic carbon detection (LC-OCD). The first fraction consisted of 95 % biopolymers, the second fraction contained 93 % of humic substances and their building blocks and the last fraction had 87 % of LMW compounds. The study concluded that biopolymers were the major foulants in seawater reverse osmosis systems, followed by LMW compounds [16]. The success of this cross-flow fractionation can be attributed to the selected membrane fractionation procedure based on the LC-OCD chromatogram, unlike the arbitrarily selected membranes for dead-end cell UF fractionation. Additionally, the use of diafiltration improved the purity of the fractions.

Cross-flow fractionation has not been developed for fresh water sources to identify the organic matter precursors of DBPs formed during drinking water disinfection. Therefore, the objective of this paper was to develop a robust membrane fractionation protocol specifically for fresh waters, splitting organic matter into three fractions: a high (HMW), medium (MMW) and LMW fraction. The effectiveness of the fractionation protocol was validated using HPSEC – total organic carbon (HPSEC-TOC) analysis and a mathematical tool was created to finetune the fractionation. Freshwater samples collected across various seasons were fractionated, and the fractions were subsequently chlorinated and chloraminated to assess their reactivity towards the formation of THMs, HAAs, HANs, HAMs and nitrosamines.

2. Material and methods

2.1. Water source

Surface water from the reservoir of a drinking water treatment plant located in De Blankaart, Belgium was selected in this study for its high load of organic matter. Samples were collected once in 2021 for membrane screening, and six times over a nine-months period in 2023 for the actual fractionations. The general characteristics of this water are found in Table S1. The water was pre-filtered with a 6 μm Büchner filtration (Whatmann) followed by a 0.1/0.2 μm cross-flow microfiltration (PVDF, MF V0.1/V0.2, Synder filtration) to remove the suspended solids and stored at 4 °C in the dark until further use.

2.2. Analytical techniques

The water was characterized for conductivity and pH with a multiparameter analyzer C3020 (Consort), the UV absorbance at 254 nm (UV_{254}) with a UV–vis spectrophotometer (UV-1600PC, VWR Collection, 10 mm pathlength). The ion concentrations were measured with a 930 Compact IC Flex (Metrohm). Total non-purgeable organic carbon and inorganic carbon were measured with a Shimadzu TOC-V_{CPN}. The organic carbon concentration for the LMW fraction was measured with a Sievers® 900 detector because of its ability to measure concentrations below 1 mgC/L. High-Performance Size Exclusion Chromatography was used to determine the concentration of the HMW, MMW and LMW fractions using the method described in Laforce, Dejaeger et al. [17]. An example chromatogram with the integration ranges is shown in Figure S1.

2.3. Membrane screening – Flux pressure tests

Flux-pressure tests were performed to select the optimal membranes for the fractionations based on the retention of each fraction. The selection criterium for a UF membrane are high retention for the HMW fraction and low retention for the MMW and LMW fraction. For NF membranes, the criteria are low retention for the LMW fraction and high retention for the HMW and MMW fractions.

To carry out the flux-pressure tests, a full factorial design with two levels was implemented (*i.e.* two membranes, two pressures). Two NF membranes (Synder NFX, Synder NFW) and two UF membranes (Synder XT, Synder MT) were selected based on their pore size (Table S2). Each membrane was tested individually in the multichannel crossflow set-up (Text S1), resulting in four independent experiments per membrane type. NF and UF experiments were conducted at transmembrane pressures (TMP) ranging from 3 to 7 bar and 1 to 5 bar, respectively. The TMP was increased gradually (ΔP=1 bar) every 30 min. Samples were taken at 1 and 2 bar for UF, and at 3 and 5 bar for NF. At each TMP, samples were taken twice at 30 min intervals from the feed tank and permeate tube to verify process stability. Samples were analyzed with

the HPSEC-TOC system to calculate the retentions of each organic matter fraction. The selectivity S was calculated to determine the optimal membrane and pressure combination for effective organic matter separation. It is a general measure in several membrane applications to assess the separation of a desired compound from other compounds and is defined as ([18–20]):

$$S_{\frac{A}{B}} = \frac{\frac{C_{p,A}}{C_{p,B}}}{\frac{C_{f,A}}{C_{f,B}}} = \frac{1-R_A}{1-R_B} \quad (1)$$

$$R_i = 1 - \frac{C_p}{C_f} \quad (2)$$

Where $S_{A/B}$ is the selectivity of fraction A over B, R_A is the retention of the least retained fraction, R_B the retention of the most retained fraction, C_p is the concentration of fraction i in the permeate tube, C_f is the concentration of fraction i in the feed tank. Since selectivity has values greater than unity (Mulder) [19], the selectivity S was normalized between 0 and 1 (S_N). S_N is defined as:

$$S_{N,A/B} = 1 - \frac{1}{S_{\frac{A}{B}}} = 1 - \frac{1-R_B}{1-R_A} \quad (3)$$

When S_N=1, the two compounds are separated completely (R_B=1) when S_N=0, no separation occurs (R_A=R_B).

The normality of each dataset was tested with the Shapiro-Wilk test ($p = 0.05$). Statistical analysis was then performed with the parametric ANOVA test followed by the Fisher's Least Significant Difference test ($p = 0.05$) or the non-parametric Kruskall-Wallis test followed by the uncorrected Dunn's test ($p = 0.05$).

2.4. Mathematical tool

A mathematical tool was developed to optimize the fractionation process and to predict the necessary concentration (CF) /diafiltration factors (DF) for the individual fractionations based on the initial concentration of each fraction in the water resource (see 2.5). The input variables for the tool include the permeate flow of the membrane, the retention of each fraction, and the filtration time. The output variables include the concentration of each fraction and the composition in the concentrate and permeate at time t. The mathematical tool assumes a constant flux and retention, since severe fouling will be avoided to ensure an effective recovery of the organic matter during the fractionation process.

The tool consists of 2 equations:

$$\ln\frac{C_{f,t}}{C_{f,0}} = -R^{*}\ln\left(1 - \frac{Q_p}{V_0}{}^{*}t\right) \text{ during normal filtration} \quad (4)$$

$$\ln\frac{C_{f,t}}{C_{f,0}} = (R-1)\frac{Q_p}{V_0}{}^{*}t \text{ during diafiltration} \quad (5)$$

With $C_{f,t}$ representing the concentration of a certain fraction at time t in the feed tank (mgC/L), $C_{f,0}$ the initial concentration of a certain fraction in the feed tank (mgC/L), R the retention of that fraction (−), Q_p the permeate flowrate (L/h), V_0 the volume of the feed tank at t = 0 (L). Both the retention and the permeate flowrate are assumed to be constant.

The performance of the tool was validated using a salt solution that mimics an average salt composition of surface water. This salt solution contained 130 mg/L $MgSO_4{\cdot}7H_2O$, 213.7 mg/L $CaCl_2{\cdot}2H_2O$, 76.8 mg/L $KHCO_3$ and 365.4 mg/L $NaHCO_3$ in MilliQ (Merck). A NF experiment (NF270, Dow) was conducted at 4 bar TMP using the single-channel set-up (Text S1). The NF270 membrane was selected due to known salt retentions from previous experiments (results not shown). The filtration process included 1 h of concentration followed by 2 h of diafiltration. Samples were taken every 15 min from the feed tank, permeate tank and permeate tube, and analyzed using ion chromatography. The experimentally determined concentrations in the feed and permeate tanks were compared with the predicted concentrations. The experiment was conducted twice with new membrane coupons.

After the validation, the mathematical tool was used for simulations to determine the optimal conditions for achieving the purest fractions. The parameters varied in the simulation included the CF (2, 4, 8), DF (4, 8, 12) and configuration (NF before/after UF) (Fig. 1). The average flux and retentions for the HMW, MMW and LMW fractions from the membrane screening (see 3.1) were used as input variables in the mathematical tool along with the minimum, maximum and average concentrations of the fractions measured in this study.

2.5. The fractionation experiments

Based on the fractionation development and the mathematical tool, the configuration with UF positioned before NF was chosen for the actual fractionation experiments (Fig. 1A, see 3.1, 3.2). Fractionations were conducted with various raw water samples from De Blankaart, collected in March, April, June, September, October and November (Table S1 for characteristics). Fresh membrane coupons were used for each fractionation and the single-channel set-up was used for the process (Text S1). In the initial fractionation step, UF (Synder XT, 2 bar TMP) was performed to isolate the MMW and LMW fractions in the permeate while retaining the HMW fraction in the concentrate. The CF for the first three fractionations (sampled in March, April, June) was set at four as predicted by the mathematical tool to be the most optimal condition (see 3.2). However, for the last three fractionations (sampled in September, October, November), a CF of two was used in an effort to minimize the loss of HMW compounds (see 3.3.3.1). Subsequently, in a second step (Fig. 1A – step 2), a diafiltration was conducted to remove residual compounds of the MMW and LMW fractions from the UF retentate. For this purpose, a salt solution resembling the salt composition of De Blankaart containing 215 mg/L $MgSO_4{\cdot}7H_2O$, 270 mg/L $CaCl_2{\cdot}2H_2O$, 300 mg/L $NaHCO_3$ and 155 mg/L $KHCO_3$ in MilliQ water, was gradually added to the feed tank at the same flowrate as the permeate flowrate. The DF was determined individually for each fractionation with the mathematical tool to ensure nearly complete removal of the MMW and LMW fractions from the UF retentate (see 3.3.3.1). Following this, the permeates from steps 1 and 2 were combined and directed to a NF unit (Synder NFW, 3 bar TMP, CF=5) to collect the LMW fraction in the permeate and the MMW fraction in the retentate (Fig. 1A – step 3).

Mass balance, recovery and osmotic pressure calculations can be found in Text S3.

2.6. Chlorine/chloramine reactivity test

A NaOCl stock solution (10–15 %) was used to chlorinate the samples. For chloramine production, 25 mM of NaOCl was added gradually to a stirred solution of 50 mM NH_4Cl adjusted to pH 10 with NaOH to avoid dichloramine formation [21]. The concentration of NH_2Cl was determined by measuring the absorbance at 245 nm (ε = 461 M^{-1} cm^{-1}), while potential dichloramine formation was measured at 294 nm (ε = 278 M^{-1} cm^{-1}).

Various Cl_2/dissolved organic carbon ratios (Cl_2/DOC) were initially tested for both chlorine and chloramine on the reservoir water to obtain a chlorine residual of 1 mgCl_2/L after 24 h in the dark (pH 7, 25 °C). This approach ensures that sufficient chlorine is added to overcome side reactions with reducing agents and ammonia. The obtained fractions were chlor(am)inated using the same Cl_2/DOC ratio as the reservoir water. Br^- and I^- concentrations were adjusted with KBr and KI in all fractions to maintain consistent Br/DOC and I/DOC-ratios. Experiments were conducted in triplicate. MilliQ water was treated equally with 1.3 mgCl_2/L in duplicate with chloramine and chlorine. The samples were quenched using ascorbic acid with a molar ratio of 1.5 ascorbic acid/Cl_2 [22]. Samples were analyzed for THMs, HAAs by head-space GC–MS and,

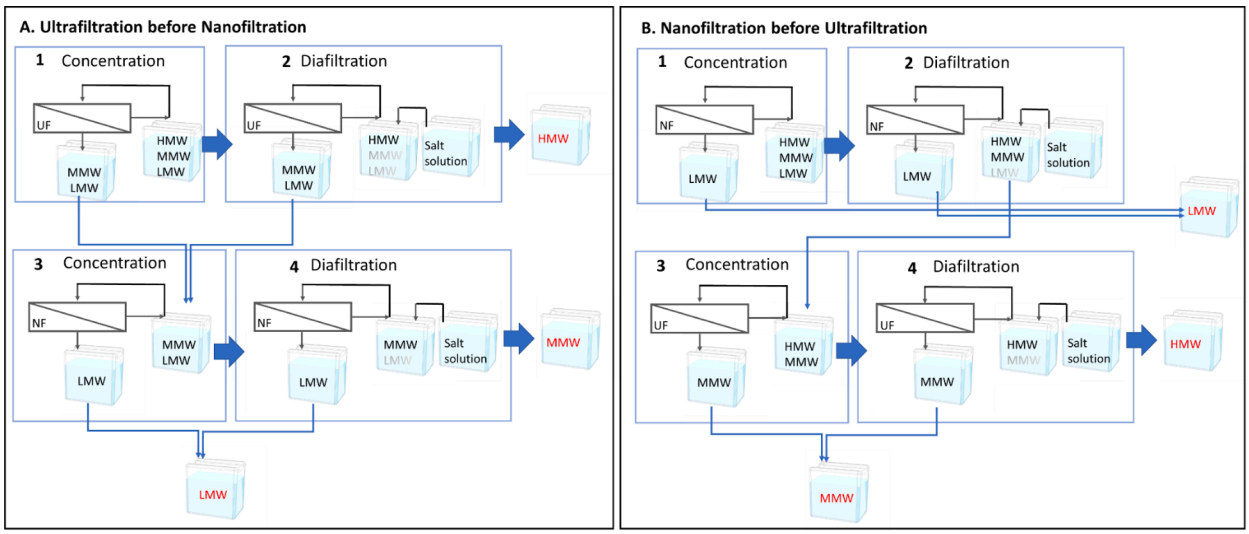

Fig. 1. Schematic representation of the membrane fractionation options. A) The high molecular weight fraction (HMW) is split from the medium (MMW) and low molecular weight fraction (LMW) using ultrafiltration (UF) and continuous diafiltration with a salt solution. The UF permeate of the two steps is sent to a nanofiltration (NF) unit to split the MMW from the LMW with a concentration and continuous diafiltration step. B) The LMW is split from the HMW and MMW using NF and continuous diafiltration with a salt solution. The NF concentrate is sent to an UF to split the HMW from the MMW with a concentration and continuous diafiltration step.

HANs, HAMs and nitrosamines by GC–MS-MS after liquid–liquid extraction. Detailed descriptions of the analytical methods can be found in the Supplementary Information, Text S4.

The specific formation potential (μg/mgC) for a fraction was calculated as:

$$DBPFP_A = \frac{\sum [DBP]_i}{[TOC]_A} \quad (6)$$

With DBPFP the specific formation potential of a DBP family in fraction A, $[DBP]_i$ the concentration of compound i of the DBP family (μg/L) and $[TOC]_A$ the total organic carbon concentration of fraction A (mgC/L).

To investigate the contribution of DBP formation coming from MMW compounds in the HMW fraction, the following equation was used:

$$DBP_{MMW} = \sum_{n=1}^{6} \left[TOC_{MMWinHMWfraction}\right]_n * DBPFP_{MMW,n} \quad (7)$$

With DBP_{MMW} the DBP formation coming from MMW compounds (μg/L), [TOC] the organic carbon concentration of the MMW compounds in the HMW fraction (mgC/L), $DBPFP_{MMW}$, the specific DBP formation potential from the MMW fraction (μg/mgC) and n the number of sampling rounds. The DBP_{MMW} was then compared to the total DBP formation from the HMW fraction.

3. Results and discussion

3.1. Membrane selection

Two UF membranes were evaluated with surface water from De Blankaart for their effectiveness to separate the HMW fraction (>20 kDa) from the MMW fraction (0.3 – 20 kDa), while two NF membranes were evaluated to separate the MMW fraction from the LMW fraction (<0.3 kDa) as measured through HPSEC-TOC. The selection criteria for a UF membrane were based on its ability to display a high retention for the HMW fraction, whereas, NF membranes were expected to display a low retention for the LMW fraction. Synder XT and Synder NFW were selected based on their performances reported by Yin, Li et al. [16], who selected these membranes as optimal membranes for NOM fractionation in seawater. Synder MT was included in this study based on its higher MWCO of 5 kDa (Table S2), compared to Synder XT, which should promote the passage of the MMW fraction while still retaining the HMW fraction (>20 kDa). On the other hand, Synder NFX was selected for its lower MWCO (150 - 300 Da, Table S2) in contrast to Synder NFW, to prevent passage of the MMW fraction (>0.3 kDa). Their actual MWCOs were calculated by fitting the retention of each PEG-solution to the log-normal model (Table S2, Figure S3, Text S2). Overall, the calculated MWCOs were found to be lower than those reported by the manufacturer. This difference was ascribed to unspecified testing conditions and methodologies by the manufacturer, which may lead to variations in MWCO-values as reported by Causserand, Pierre et al. [23].

Flux-pressure tests were conducted to screen the membranes. For the UF membranes, the flux increased linearly with TMP up to 4 bar. At 5 bar, the critical flux was reached, since the flux does not increase substantially beyond this point, especially for the MT membrane (Fig. 2). The critical flux is defined as the point where fouling becomes dominant [24]. For the NF membranes, flux increased linearly with TMP across the entire pressure-range. S_N was determined at TMPs well below the critical flux (1–2 bar for UF and 3–5 bar for NF). There was no difference in selectivity between 1 and 2 bar for the MT membrane, but a significant increase of S_N was observed from 1 to 2 bar for the XT membrane (Fig. 2). This is because the retention of the HMW fraction significantly increased with TMP while the retention of the MMW decreased for the XT membrane. Additionally, the retention of the MMW fraction in the MT membrane also decreased significantly with TMP.

The retention of proteins and other charged solutes in UF systems was described previously using a stagnant film model [25]. Generally, a higher flux results in more concentration polarization at the membrane surface. Moreover, the convective flux becomes more dominant compared to the diffusive flux, resulting in a decreased retention [25]. The observed decrease in retention at increasing fluxes for the MMW fraction, consisting of negatively charged humic substances [26], is explained by this phenomenon, since the negative electrostatic repulsion is counterbalanced by the increased concentration polarization and convective flux. The increased retention for the HMW fraction with TMP (and flux), is less straightforward. It can be expected that the concentration polarization induced more adsorption of biopolymers (contained in the HMW fraction) on the membrane surface, since biopolymers have been identified as having the highest fouling potential for MF and UF [17,27]. The average S_N of the XT membrane at 2 bar is 0.91, making this membrane a suitable candidate for the separation of the HMW and

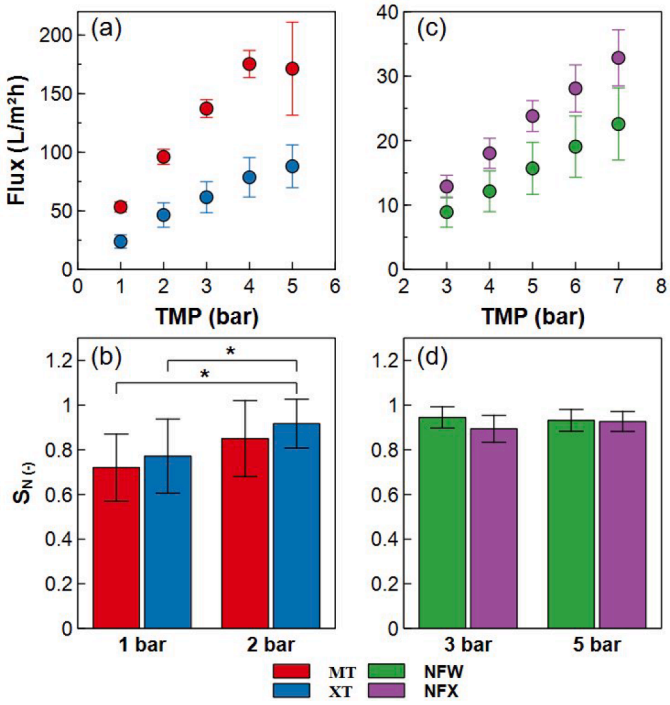

Fig. 2. (a,c) Flux (L/m^{2}h) versus transmembrane pressure (TMP, bar) of 2 ultrafiltration membranes ((a) Synder MT (red), Synder XT (blue)) and 2 nanofiltration membranes ((c) Synder NFW (green), Synder NFX (purple)). Standard deviations originate from the fluxes of each separate membrane coupon (n = 4). (b,d) The normalized selectivity (S_N) versus TMP (bar), calculated from the retention of high and medium molecular weight fraction in (b) and from the retention of medium and low molecular weight fraction in (d). Standard deviations originate from different membrane couons (n = 4). Statistical differences are marked with * ($p < 0.05$).

MMW fractions.

For the NF membranes, all the fluxes increased linearly with TMP, indicating that no critical flux was reached. The S_N were all very high (>0.9) and not significantly different from each other. The MWCOs from these membranes were found to be very similar (130 *vs.* 139 Da), despite the more distinct values reported by the manufacturer (Table S2). The four tested conditions could therefore be used for the actual fractionation process. For continuity, the condition with the highest average S_N was chosen, *i.e.* the NFW membrane at 3 bar.

3.2. Mathematical tool for fractionation process design

A mathematical tool was developed in the first place to design the fractionation process (membrane order, CF, DF). In a next stage (see 3.3.3.1), it was used to select the necessary DF based on the organic matter composition of the starting water to enhance a good separation of the different fractions and predict it beforehand. The performance of the tool was first validated by performing NF separation of a synthetic salt solution. The salt retentions and flux (both input parameters of the mathematical tool) of the NF membrane were already acquired from previous experiments. The experimentally observed concentrations in the validation experiments were compared with the predicted concentrations using the mathematical tool. The tool accurately predicted the observed concentrations in concentrate and permeate during a concentration and diafiltration step for a specific membrane (Figure S4).

Simulations were conducted using the mathematical tool to design the fractionation process to obtain the purest fractions. The tool used the average flux and retention for the HMW, MMW and LMW fractions from the membrane screening as input variables, together with the minimum, maximum and average concentrations of the three fractions measured in De Blankaart (Table S1, section 3.1). The membrane fractionation can be conducted in two ways: UF before NF or NF before UF. In both configurations, the HMW fraction should end up in the UF concentrate, the MMW fraction in the NF concentrate and the LMW fraction in the NF permeate (Fig. 1).

The mathematical tool simulated the influence of membrane configuration, CF and DF on the purity of the HMW, MMW and LMW fraction (Fig. 3). The CF did not greatly influence the final purity in each fraction. Increasing the DF increased the final purity of the HMW fraction, while decreasing the purity of the LMW fraction in both configurations. This is expected as the retention of the MMW fraction is not 100 % during NF treatment, and its concentration in the NF concentrate is much higher (5x on average) compared to the LMW fraction. The purity of the MMW fraction does not change substantially in function of DF when UF is placed before NF, but it decreases ~ 10 % when NF is placed before UF. Therefore, placing UF before NF seems the best configuration as the DF can be maximized to reach high purity of the HMW fraction, without affecting the purity of the MMW fraction. During NF, diafiltration should be avoided to reach the highest purity in the LMW fraction.

To summarize, the following methodology has been applied for the periodic fractionation experiments where UF is positioned before NF (section 3.3.3). A CF of 2 and 4 has been tested on the UF membrane since a high CF might induce fouling of the membrane, a phenomenon not included in the mathematical tool. A CF of 5 is used during NF to provide sufficient NF permeate for the chlorination experiments. To maximize the purity of the final HMW fraction, the mathematical tool was employed as a means to calculate the necessary DF for UF before each individual fractionation experiment based on the concentrations of each fraction in the initial water sample as determined by HPSEC-TOC. Finally, as stated before, no DF is executed during NF.

3.3. Periodic fractionation experiments

3.3.1. Raw water characteristics

The general characteristics of the six water samples collected from March to November 2023 are shown in Table S1. The pH, UV_{254} and inorganic carbon concentration remained relatively constant over the sampling period. The DOC concentration varied from 7.8 to 10.8 mgC/L during the sampling period with a significant change in the HMW

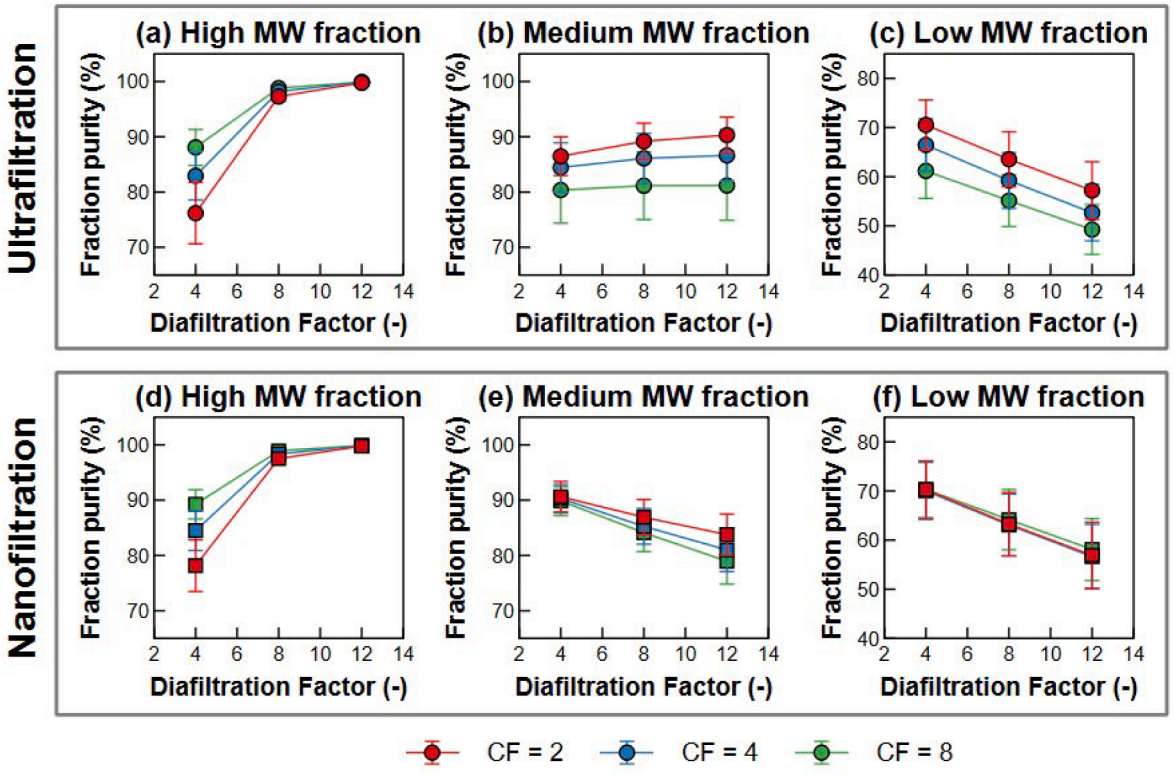

Fig. 3. Simulation results of the mathematical tool. The purity of each molecular weight (MW) fraction is presented in function of the concentration factor (CF) and diafiltration factor. (a,b,c) Ultrafiltration is executed before nanofiltration, (d,e,f) Nanofiltration is executed before ultrafiltration. Standard deviations originate from simulating the minimum, maximum and average concentrations of the fractions found in De Blankaart from 7 replicates.

fraction which doubled by the end of summer (Table S1). This increase is ascribed to the dry period during the summer of 2023, supported by the increase in ionic concentrations and the occurring algal bloom.

3.3.2. *Microfiltration pre-treatment*

Two microfiltration (MF) membranes in crossflow configuration were tested to remove the particulate matter from the water. The average pore size of the membranes were 0.1 (MF0.1) and 0.2 μm (MF0.2), as reported by the manufacturer. The MF flux declined rapidly during the first two hours for MF0.1 and dropped dramatically within the first half hour for MF0.2 (**Figure S5**). The mass balances and recoveries of each fraction in the MF permeate was better for MF0.2 compared to MF0.1 (Table 1), with the recovery of the HMW fraction being very poor for the MF0.1 membrane (<10 %). Fouling of MF membranes by colloidal organic matter containing polysaccharides and protein-like material (>50 kDa) is a well-described phenomenon. The loss in HMW fraction (>20 kDa) with both MF0.1 and MF0.2 was therefore ascribed to the higher fouling potential of this fraction [28,29]. The lower recovery of the HMW fraction with the MF0.1 membrane probably occurs from the smaller pore size, resulting in the formation of a thicker cake layer and thereby a higher retention of the HMW fraction. The MF0.2 membrane was therefore selected to pre-treat the water to avoid excessive loss of HMW. The mass balances and recoveries for all the performed MF treatments for the individual fractionations are found in Table S3.

Table 1
Mass balance and recovery$_{MF}$ (%) for the high (HMW), medium (MMW) and low molecular weight (LMW) fractions (n = 2).

	MF0.1	MF0.2	MF0.1	MF0.2
	Mass Balance (%)		*Recovery$_{MF}$ (%)*	
HMW fraction	65.0 ± 5.66	66.0 ± 11.3	7.95 ± 2.19	28.5 ± 6.36
MMW fraction	98.0 ± 2.83	101 ± 12.0	85.5 ± 0.707	89.5 ± 10.6
LMW fraction	101 ± 17.0	109 ± 14.1	96.5 ± 16.3	99.5 ± 4.95

3.3.3. *Fractionation*

3.3.3.1. Ultrafiltration. Six sampling rounds were conducted at De Blankaart reservoir in March, April, June, September, October and November. The first three water samples were fractionated using a CF of 4 during UF, while the last three water samples used a CF of 2 to reduce the loss of HMW compounds (see further). The DF for UF was calculated separately for each individual fractionation experiment with the mathematical tool to maximize the purity of the HMW fraction, since the concentration of the different fractions in the feed differed over time (Table S1, Table S4). The selected DF for each fractionation experiment was set at the point where less than 0.05 mgC/L of the MMW fraction remained in the UF concentrate, at which point the LMW fraction was already completely removed.

The actual DFs differed substantially from the DFs suggested by the mathematical tool for the third and last two fractionations (Table S4). This is because the actual diafiltration volume that needed to be added for the last three fractionations (CF=2) was almost twice as high as for the first three fractionations (CF=4, Table S4). Since the LMW fraction is washed out much quicker than the MMW fraction from the UF concentrate, the actual diafiltration volume was reduced in these cases to limit the dilution of the LMW fraction in the UF permeate (which occurred in the fourth fractionation). For the third fractionation, the membrane flux was unexpectedly low, resulting in an earlier stop of the diafiltration due to time constraints.

The ultrapure water used for the diafiltration step was supplemented with $CaCl_2$, $MgSO_4$, $NaHCO_3$ and $KHCO_3$ to mimic the ionic environment of the raw water. Without the adjustment, the retention of the MMW fraction (having negatively charged compounds) increased substantially during the diafiltration (data not shown) which was not

conducive in removing the MMW from the UF concentrate. The adjustment of electrical conductivity and especially calcium levels was previously identified as important in literature as well [30].

The UF flux decreased over time during the first step (concentration) at a CF of 4 (Fig. 4a), while it remained constant during a CF of 2 (Fig. 4b). As expected at a higher CF, there was more concentration polarization and adsorption onto the membrane, resulting in flux decline. However, no significant differences were found in the mass balances for the three fractions between a CF of 4 and a CF of 2 (Table 2). Particularly, there was a loss in compounds of the HMW fraction during this step at both CFs. Biopolymers with high MW (>100 kDa) have been identified to have the highest fouling potential in low-pressure membrane systems such as MF and UF [27]. It was therefore inevitable that some compounds of the HMW fraction adsorbed onto the membrane surface. During diafiltration, the flux remained relatively constant, with slight increases during fractionation 2, 3 and 6 and a small decrease during fractionation 1, 4 and 5 (Fig. 4**c,d**). These variations can be explained by differences in osmotic pressure over the membrane (Table S5).

There is no significant difference in HMW fraction recovery rate between a CF of 4 and a CF of 2 (Table 2, 44.0 % ± 21.2 % *vs.* 46.7 % ± 12.9 %). A complete removal of the LMW fraction from the UF concentrate was achieved in all fractionations as predicted by the mathematical tool. For the MMW fraction, the recovery rate was less than 3 % in the UF concentrate after diafiltration for fractionations 1, 2 and 4, indicating efficient removal from the HMW fraction. The higher recovery rates (>5 %) for the other three fractionations were due to the lower actual diafiltration volume that was used compared to the model calculations (Table S4). This shows the added value of the mathematical tool to determine the DF needed for each specific water sample to be fractionated to achieve effective isolation of the HMW fraction.

Table 2
Mass balances (%) and final recovery (%) after UF concentration and diafiltration of the high (HMW), medium (MMW) and low molecular weight (LMW) fractions for a concentration factor (CF) of 4 and 2.

Fractionation n°	CF=4			CF=2		
	1	*2*	*3*	*4*	*5*	*6*
	Mass Balance concentration step (%)					
HMW fraction	62	55	95	67	103	51
MMW fraction	98	98	99	96	94	76
LMW fraction	96	101	100	99	88	97
	Mass Balance diafiltration (%)					
HMW fraction	58	52	71	77	55	62
MMW fraction	70	89	89	100	98	102
	Recovery in UF concentrate (%)					
HMW fraction	36	28	68	52	56	32
MMW fraction	2	2	9	3	6	7
LMW fraction	0	0	0	0	0	0

However, even for fractionations 1, 2 and 4, where the actual and theoretical DFs were similar, a concentration between 0.3 and 0.45 mgC/L of the MMW fraction was left in the UF concentrate, which is higher than was predicted by the mathematical tool (<0.05 mgC/L). The MMW fraction comprises compounds between 0.3 – 20 kDa and the HPSEC-TOC chromatograms of the UF concentrate clearly show that particularly the higher MW compounds from the MMW fraction were still present in the HMW fraction (Figure S6). The retention used in the mathematical tool is an average for the entire MMW fraction, but it is evident that smaller compounds in this fraction are more easily removed during diafiltration than larger compounds. Therefore, there seems to be a limit to the MW of the compounds in the MMW fraction that can be effectively removed during diafiltration in this system. This limit is

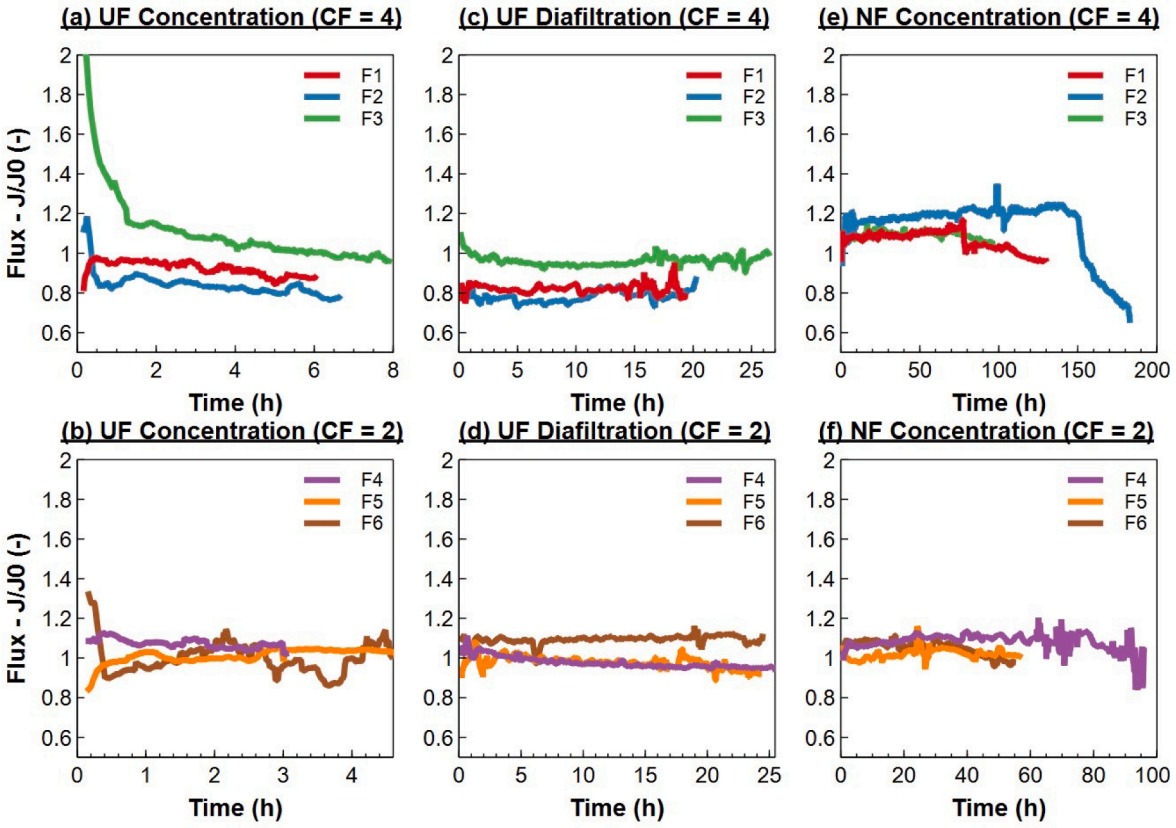

Fig. 4. Flux (J/J_0) versus time (h) in ultrafiltration (UF) concentration step with (a) a concentration factor (CF) of 4 followed by (c) diafiltration and (e) nanofiltration (NF) or with (b) a concentration factor of 2 followed by (d) diafiltration and (e) NF. F1-6 indicate the 6 individual executed fractionations over a 9-months period.

reflected in the composition of the UF concentrate, where a maximum of 50/50 HMW/MMW compounds could be achieved with fractionations 1 and 2 (Fig. 5).

The removal of the MMW fraction for the waters with a CF of 2 was more challenging. Concentrating the MMW fraction at a CF of 2 resulted in a lower concentration gradient over the membrane surface during diafiltration compared to a CF of 4, necessitating a doubled diafiltration volume (Table S4). Nonetheless, more compounds of the MMW fraction seemed to adsorb onto the membrane surface during diafiltration of the first three fractionations (CF=4) as seen from the incomplete mass balances compared to the last three fractionations (CF=2), although this was not statistically significant (Table 2, 82.7 % ± 11.0 % *vs.* 100 % ± 2.0 %).

Overall, the use of a CF of 4 did not result in a greater loss of compounds from the HMW and MMW fractions compared to a CF of 2 although a small decrease in flux was seen at a CF of 4. A CF of 4 also required less diafiltration volume to effectively remove the MMW and LMW fractions from the UF concentrate, therefore also minimizing dilution of the LMW fraction in the UF permeate. Therefore, a CF of 4 is preferred to perform the fractionations.

3.3.3.2. Nanofiltration. The permeate streams from the UF concentration and diafiltration steps were combined and directed to a NF membrane to separate the LMW fraction from the MMW fraction (Fig. 1A). Again, a difference in flux characteristics was observed between the fractionations. The clean water fluxes (measured with demineralized water) from the membrane coupons used in fractionations 4, 5 and 6 were higher (7.7 – 16.3 – 17.3 L/m^{2}h) compared to those used in fractionations 1, 2 and 3 (6.1 – 3.3 – 7.4 L/m^{2}h). The higher flux, which probably stems from a less dense membrane structure in those specific coupons, resulted in a lower osmotic pressure difference due to the higher salt passage over the membrane (Table S5). Therefore, a lower flux decline was observed over time (Fig. 4). The significant flux decline during fractionation 2 was caused by the very low clean water flux (3.3 L/m^{2}h) of that particular membrane coupon, resulting in higher retention of the compounds and subsequent fouling. This was also clear from the incomplete mass balances of the MMW and LMW fractions for this fractionation, while other fractionations resulted in closed mass balances (Table 3). Also, incomplete mass balances were observed for calcium together with inorganic carbon or sulfate in nearly all fractionations (Table S6). The saturation indexes clearly indicate that calcium carbonate precipitation has occurred partially leading to flux decline in the fractionations (Table S7).

Table 3
Mass balances (%) of the medium (MMW) and low molecular weight (LMW) fractions after nanofiltration (NF) for the six fractionations, the final recovery (%) in the NF concentrate and the final LMW concentration in the NF permeate (mgC/L).

Fractionation n°	*1*	*2*	*3*	*4*	*5*	*6*
	Mass Balance (%)					
MMW fraction	90	83	92	98	97	92
LMW fraction	99	87	103	116	91	103
	Recovery NF concentrate (%)					
MMW fraction	74	74	71	87	82	82
LMW fraction	95	81	103	114	66	102
	LMW concentration in NF permeate (mgC/L)					
	0.288	0.337	0.592	0.188	0.303	0.173

The final composition in the NF concentrate (Fig. 5) was not significantly different from the initial water composition, except for the absence of the HMW fraction. Complete removal of the LMW fraction was not possible without diafiltration. Diafiltration would require a DF between 18 and 27 to obtain a LMW fraction < 0.05 mgC/L in the NF concentrate. This would correspond to a volume of 47 – 64 L or a duration of 300 to 2000 h to finish the diafiltration, making it ineffective due to the high retention of the LMW fraction. Furthermore, as calculated by the mathematical model, it would decrease the purity of the LMW fraction (Fig. 3).

In the NF permeate, concentrations between 0.17 and 0.60 mgC/L were found by offline DOC measurements, presumably consisting only of LMW compounds (Table 3). However, this could not be directly confirmed by HPSEC-TOC because the LMW fraction appears as a tail in the chromatogram, causing the 0.17 – 0.60 mgC/L to be spread out over a 30 min timespan, which made it challenging to detect and quantify since the system has a quantification limit of 0.063 mgC/L [17]. However, no peaks in the MMW fraction could be detected either proving its purity.

Separation of MMW and LMW compounds in fresh waters with NF appeared to be challenging. Zhang, He et al. [31] tested several NF membranes with a MWCO between 370 – 1260 Da for their performance to reject DOM at 6 bar in a lab-scale set-up. Although the membranes

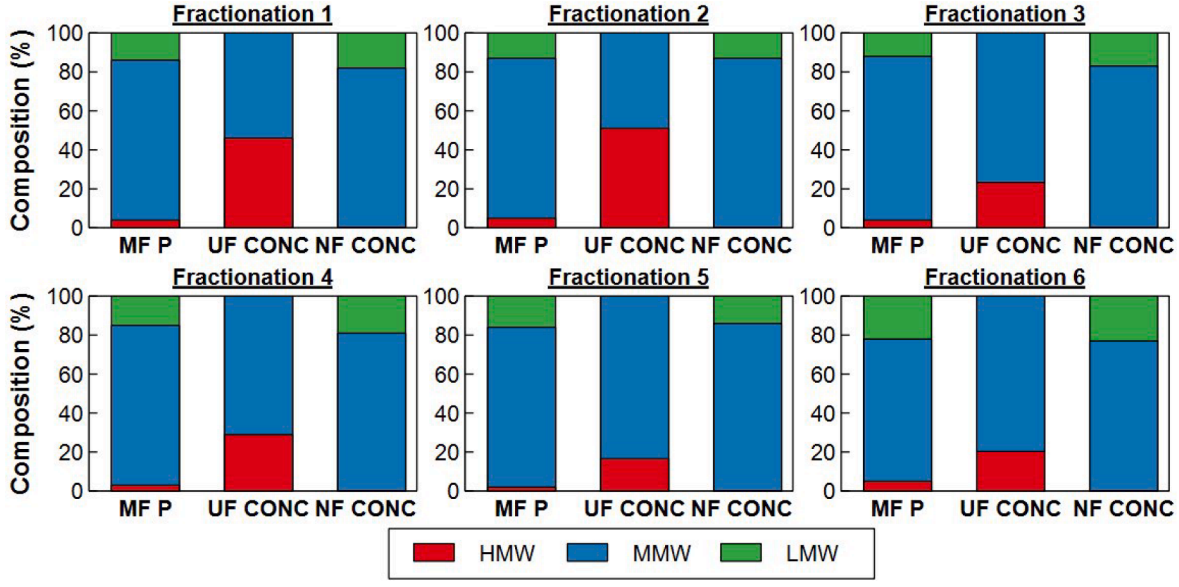

Fig. 5. Relative composition based on HPSEC-TOC analysis (%) of the high (HMW, red), medium (MMW, blue) and low molecular weight (LMW) fractions (green) in the microfiltration permeate (MF P), ultrafiltration concentrate (UF CONC) and nanofiltration concentrate (NF CONC) after fractionation 1 to 6.

showed high efficiency to reject the HMW fraction, compounds up to 5 kDa (*i.e.* part of the MMW fraction in this study) were detected in the NF permeate of the densest membrane (370 Da). It was clear from the results that the higher the MWCO, the higher the passage of molecules with MW up to 10 kDa. For this membrane fractionation, despite the low recovery of the LMW fraction in the NF permeate, it was decided to use this very dense membrane (139 Da), since no compounds from the MMW fraction would pass the membrane. However, if the recovery of the LMW

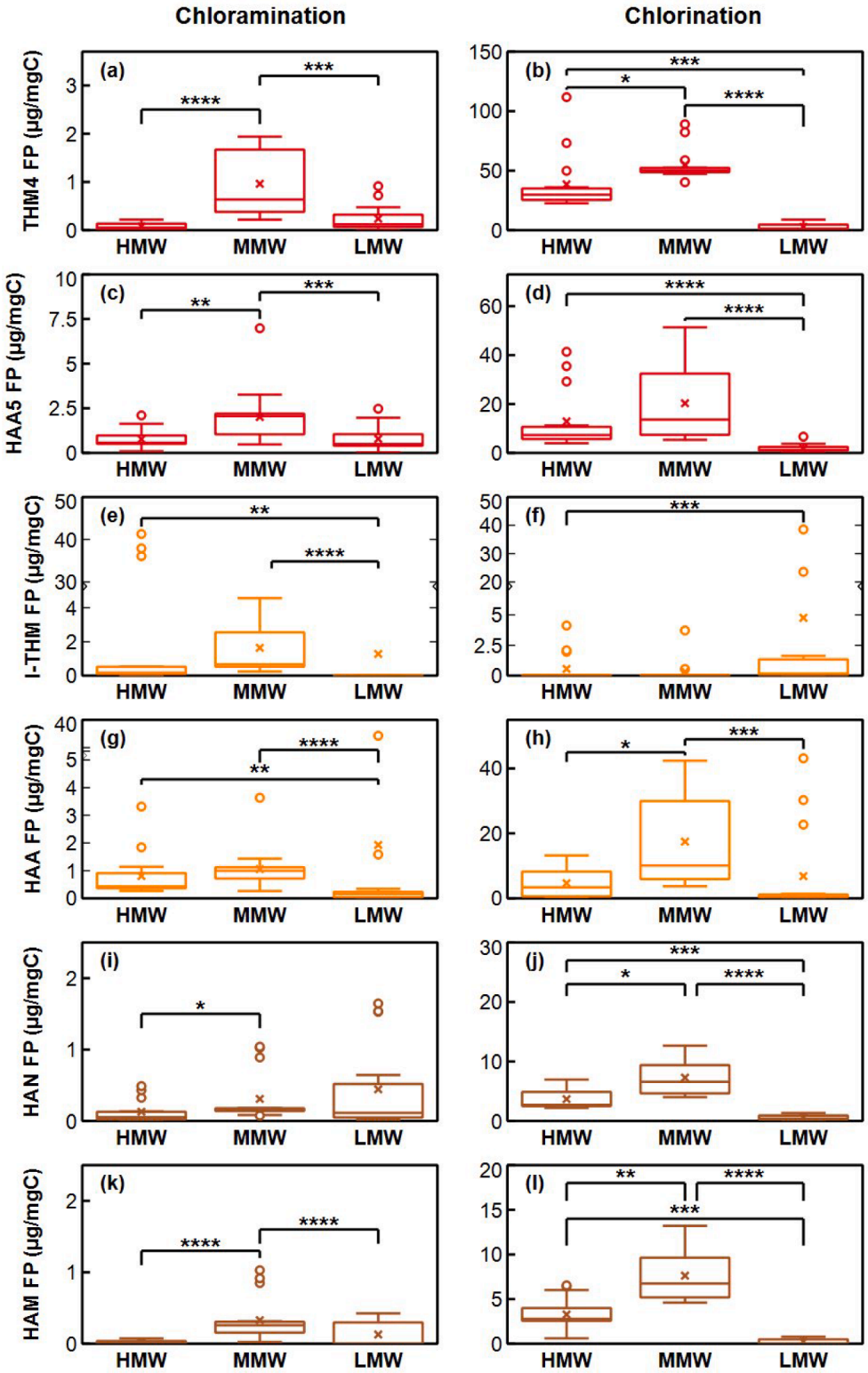

Fig. 6. Disinfection by-product formation potential (FP, µg/mgC) of regulated trihalomethanes (THM4, a,b) and haloacetic acids (HAA5, c,d), unregulated iodinated trihalomethanes (I-THM, e,f) and haloacetic acids (HAA, g,h), nitrogenous haloacetonitriles (HAN, i,j) and nitrogenous haloacetamides (HAM, k,l) in the high (HMW), medium (MMW) and low molecular weight (LMW) fraction after chloramination and chlorination. $p \leq 0.05$ (*), $p \leq 0.01$ (**), $p \leq 0.001$ (***), $p \leq 0.0001$ (****).

fraction was more important, a looser NF membrane might be a better option.

3.4. Organic matter reactivity potential towards the formation of disinfection by-products

The membrane fractions obtained from the six fractionation experiments (Fig. 1A, Fig. 5), sampled and conducted between March and November 2023, were chlorinated and chloraminated to assess their reactivity potential towards disinfection by-product formation (expressed in μg DBP/mgC, Fig. 6). Low chlorine residual (1 $mgCl_2$/L) and short reaction times (24 h) were used to simulate the conditions within a drinking water distribution system. The total organic carbon, bromide and iodide corrected concentrations in each fraction are shown in Table S8. Nitrosamines were not detected in any of the sampling rounds.

Fig. 6a, b and Fig. 6c, d show the overall specific formation potential of regulated THMs, *i.e.* THM4 and regulated HAAs, *i.e.* HAA5 from all the fractionation experiments where the MMW fraction showed the highest reactivity potential towards THM4 and HAA5 during chlorination and chloramination. However, for unregulated iodinated THM formation potentials (I-THMs, Fig. 6e, f), the LMW fraction appeared to be the most reactive during chlorination, while showing almost no reactivity during chloramination. Furthermore, the reactivity potential for I-THMs was not significantly different between the HMW and MMW fraction during chloramination. Regarding unregulated HAAs, the MMW fraction again showed the highest reactivity potential during chloramination and chlorination (Fig. 6g,h). The HMW fraction appeared equally reactive compared to the MMW fraction for HAA5 during chlorination and for unregulated HAAs during chloramination. For the HANs and HAMs belonging to the nitrogenous DBP families, the LMW fraction showed the highest reactivity potential for HANs during chloramination, while the MMW fraction showed the highest reactivity for HAN and HAM during chlorination (Fig. 6i,j,k,l).

The observed high reactivity of the MMW fraction, mostly containing humic substances, is well known and aligns with the results from resin fractionation [17], where relatively more hydrophobic compounds were found to contribute 10–20 % more towards THM and HAA formation compared to hydrophilic compounds, using similar chlorine dose and reaction time as in this study. For nitrogenous DBPs, hydrophilic compounds have been identified as the major precursor during chlorination [11]. Surrogate analysis showed that HANs can be formed from free amino acids, proteinaceous material, and combined amino acids bound to humic substances [32]. Furthermore, aromatic model compounds such as phenol and resorcinol have high reactivity towards HAM and HAN formation during chloramination [33,34]. These observations might explain the high reactivity observed in the MMW fraction for HAN and HAM formation during fast reaction with chlorine, while the similar reactivity between MMW and LMW fractions for HANs during chloramination may originate from slower and comparable reaction rates of aromatic moieties, free and bound amino acids with chloramine [32–34].

To clearly assess the role of each organic fraction, the presence of MMW compounds (2–9 % of the initial amount and 50–80 % on carbon content) in the HMW fraction has to be considered (Table 2, Fig. 5). To investigate this, the actual DBP concentration in the HMW fraction was compared to the DBP concentration that would be obtained if the reactivity in the HMW fraction came only from the MMW compounds (Equation (13), Table S9). From this calculation, it appeared that considering the I-THMs, the high formation potential found in the HMW fraction did not come from the MMW compounds within that fraction, since the concentration of I-THMs in the HMW fraction was much higher compared to the one that could have been formed from MMW compounds after chloramination (Table S9). However, in many other cases (Table S9), the concentration of formed DBPs in the HMW fraction was much lower compared to the concentration coming from the MMW compounds, which is inconsistent if the MMW compounds inside the HMW and MMW fractions have equal reactivities. The MMW compounds in the water ranged from 0.3 to 20 kDa and as shown in Figure S6, only MMW compounds with higher MW were found in the HMW fraction. Therefore, it can be concluded that the larger compounds in the HMW fraction generally had a lower reactivity potential towards most DBPs than the smaller compounds in the MMW fraction. This has significant implications for drinking water treatment plants aiming to reduce DBP precursors, since coagulation, a common drinking water treatment step, more efficiently removes large, hydrophobic compounds compared to smaller hydrophilic compounds [35].

Besides the overall differences in DBP formation potential between the different fractions, distinct seasonal variation in reactivities throughout the year were observed (Figure S7). During chlorination, the reactivity towards THM4 and HAA5 formation were similar for the HMW and MMW fractions in colder periods (April and November in Figure S7). However, the MMW fraction became more reactive compared to HMW fraction in warmer periods (June, September in Figure S7). The formation of HANs and HAMs during chlorination remained relatively constant throughout the year, with a high formation in October for both the HMW and MMW fraction.

These findings show for the first time clear seasonal variations in DBP formation between size-based fractions. In a next stage, the membrane fractions could be further characterized using more advanced characterization techniques to provide deeper insights into the molecular characteristics of the different DBP precursors.

4. Conclusions

This work successfully developed a robust crossflow membrane fractionation protocol to fractionate organic matter from freshwater sources at different times of the year into three fractions as measured with high performance-size exclusion chromatography-total organic carbon analysis. This was achieved through the following steps:

- A membrane screening showed that a tight ultrafiltration and nanofiltration membrane are the best to achieve a good separation of the three fractions with normalized selectivity factors of 0.9.
- The development of a mathematical tool facilitated the design of the membrane fractionation process showing that ultrafiltration should be placed before nanofiltration and that the concentration factor should be maximized. Moreover, the mathematical tool was used during the individual fractionation experiments to predict the necessary diafiltration factor based on the composition of the initial water to maximize the purity of the high molecular weight fraction.
- The individual fractionation experiments successfully yielded a high molecular weight fraction enriched in high molecular weight compounds (going from 3 % in the raw water to 31 % in the high molecular weight fraction on average), a medium molecular weight fraction containing 83 % medium molecular weight compounds, and a low molecular weight fraction only consisting of low molecular weight compounds.

The membrane fractions showed clear differences in disinfection by-product formation potentials after chlor(am)ination, together with variable reactivities on a seasonal basis, an outcome not reported before. Moreover, the high molecular weight fraction had overall a lower reactivity towards disinfection by-products having implications for drinking water treatment, since coagulation, a common drinking water treatment step more efficiently removes bigger molecules which have been shown in this study to be less important for disinfection by-product formation. These results are of great relevance to drinking water companies, as they enable the monitoring of DOM composition (changes) throughout the year and during the water treatment using routine HPSEC-TOC analysis. This, in turn, allows for the prediction of potential DBP formation as identified in this study. Such insights will be important

to manage the production of various disinfection by-products in tap water, particularly as freshwater treatment becomes increasingly challenging due to changes in organic matter concentration and composition driven by climate change and growing human activities.

CRediT authorship contribution statement

Karlien Dejaeger: Methodology, Validation, Formal analysis, Investigation, Data curation, Writing – original draft, Writing – review & editing, Visualization. **Marjolein Vanoppen:** Conceptualization, Resources, Writing – review & editing, Supervision, Project administration. **Justine Criquet:** Conceptualization, Resources, Writing – review & editing, Supervision, Project administration, Funding acquisition. **Gabriel Billon:** Resources, Writing – review & editing, Supervision, Project administration, Funding acquisition. **Cécile Vignal:** Resources, Writing – review & editing, Supervision, Project administration, Funding acquisition. **Emile R. Cornelissen:** Conceptualization, Methodology, Resources, Writing – review & editing, Supervision, Project administration, Funding acquisition.

Declaration of competing interest

The authors declare that they have no known competing financial interests or personal relationships that could have appeared to influence the work reported in this paper.

Data availability

Data will be made available on request.

Acknowledgements

This project has received funding from the European Union's Horizon 2020 research and innovation program under the Marie Sklodowska-Curie grant agreement [No 847568]. We would like to thank De Watergroep and especially Klaas Schoutteten and Veerle D'Haeseleer for providing water samples.

Professor Emile Cornelissen would like to acknowledge the FWO-SBO Biostable Project [S006221N]. The Region Hauts-de-France and the French government are warmly acknowledged through the founding of the CPER ECRIN. Justine Criquet would like to acknowledge the French national Research Agency Agence Nationale de la Recherche (ANR) - NOMIC projet [ANR-21-CE04-0003-01].

Appendix A. Supplementary material

Supplementary data to this article can be found online at https://doi.org/10.1016/j.seppur.2024.129635.

References

[1] Fawell, J.K., et al., *Drinking water quality and health.* Pollution: Causes, effects and control, 2004.
[2] M. Diana, et al., Disinfection byproducts potentially responsible for the association between chlorinated drinking water and bladder cancer: A review, Water Res. 162 (2019) 492–504, https://doi.org/10.1016/j.watres.2019.07.014.
[3] C.M. Villanueva, et al., Exposure to widespread drinking water chemicals, blood inflammation markers, and colorectal cancer, Environ. Int. 157 (2021) 106873, https://doi.org/10.1016/j.envint.2021.106873.
[4] Council, D.o.t.E.P.a.o.t., *The European Parliament - Directive of the European Parliament and of the Council on the quality of water intended for human consumption (recast)* 2020, PE-CONS 53/20.
[5] B. Chen, et al., Methods for total organic halogen (TOX) analysis in water: Past, present, and future, Chem. Eng. J. 399 (2020) 125675, https://doi.org/10.1016/j.cej.2020.125675.
[6] E.D. Wagner, et al., CHO cell cytotoxicity and genotoxicity analyses of disinfection by-products: An updated review, J. Environ. Sci. 58 (2017) 64–76, https://doi.org/10.1016/j.jes.2017.04.021.
[7] Criquet, J., et al., *Chapter Five - Influence of bromide and iodide on the formation of disinfection by-products in drinking water treatment*, in *Comprehensive Analytical Chemistry*, T. Manasfi, et al., Editors. 2021, Elsevier. p. 113-134. Doi: 10.1016/bs.coac.2021.01.004.
[8] J.A. Leenheer, et al., Peer reviewed: Characterizing aquatic dissolved organic matter, Environ. Sci. Tech. 37 (1) (2003) 18A–26A, https://doi.org/10.1021/es032333c.
[9] M. Kitis, et al., Probing reactivity of dissolved organic matter for disinfection by-product formation using XAD-8 resin adsorption and ultrafiltration fractionation, Water Res. 36 (15) (2002) 3834–3848, https://doi.org/10.1016/S0043-1354(02)00094-5.
[10] L. Lin, et al., A comparison of carbonaceous, nitrogenous and iodinated disinfection by-products formation potential in different dissolved organic fractions and their reduction in drinking water treatment processes, Sep. Purif. Technol. 133 (2014) 82–90, https://doi.org/10.1016/j.seppur.2014.06.046.
[11] K. Dejaeger, et al., Identification of disinfection by-product precursors by natural organic matter fractionation: A review, Environ. Chem. Lett. (2022), https://doi.org/10.1007/s10311-022-01478-x.
[12] A. Matilainen, et al., An overview of the methods used in the characterisation of natural organic matter (NOM) in relation to drinking water treatment, Chemosphere 83 (11) (2011) 1431–1442, https://doi.org/10.1016/j.chemosphere.2011.01.018.
[13] S. Assemi, et al., Characterization of natural organic matter fractions separated by ultrafiltration using flow field-flow fractionation, Water Res. 38 (6) (2004) 1467–1476, https://doi.org/10.1016/j.watres.2003.11.031.
[14] Goslan, E.H., et al., *Natural organic matter fractionation: XAD resins versus UF membranes. An investigation into THM formation*, in *4th World Water Congress: Innovation in Drinking Water Treatment*, P. Wilderer, Editor. 2004. p. 113-119. Doi: 10.2166/ws.2004.0099.
[15] Z.Y. Zhao, et al., Disinfection characteristics of the dissolved organic fractions at several stages of a conventional drinking water treatment plant in Southern China, J. Hazard. Mater. 172 (2–3) (2009) 1093–1099, https://doi.org/10.1016/j.jhazmat.2009.07.101.
[16] W. Yin, et al., Fouling behavior of isolated dissolved organic fractions from seawater in reverse osmosis (RO) desalination process, Water Res. 159 (2019) 385–396, https://doi.org/10.1016/j.watres.2019.05.038.
[17] E. Laforce, et al., Thorough validation of optimized size exclusion chromatography-total organic carbon analysis for natural organic matter in fresh waters, Molecules 29 (9) (2024) 2075, https://doi.org/10.3390/molecules29092075.
[18] A. Mehta, et al., Permeability and selectivity analysis for ultrafiltration membranes, J. Membr. Sci. 249 (1) (2005) 245–249, https://doi.org/10.1016/j.memsci.2004.09.040.
[19] J. Mulder, et al., Basic Principles of Membrane Technology, Springer, Netherlands, 1991.
[20] Park, H.B., et al., *Maximizing the right stuff: The trade-off between membrane permeability and selectivity.* Science, 2017. **356**(6343): p. eaab0530. doi:10.1126/science.aab0530.
[21] Lee, W., et al., *Erratum to "Comparison of colorimetric and membrane introduction mass spectrometry techniques for chloramine analysis": [Water Res. 41 (2007) 14].* Water Research, 2007. **41**(18): p. 4271. Doi: 10.1016/j.watres.2007.07.015.
[22] N. Moore, et al., A comparison of sodium sulfite, ammonium chloride, and ascorbic acid for quenching chlorine prior to disinfection byproduct analysis, Water Supply 21 (5) (2021) 2313–2323, https://doi.org/10.2166/ws.2021.059.
[23] C. Causserand, et al., Characterization of ultrafiltration membranes by tracer's retention: Comparison of methods sensitivity and reproducibility, Desalination 250 (2) (2010) 767–772, https://doi.org/10.1016/j.desal.2008.11.038.
[24] P. Bacchin, et al., Critical and sustainable fluxes: theory, experiments and applications, J. Membr. Sci. 281 (1–2) (2006) 42–69, https://doi.org/10.1016/j.memsci.2006.04.014.
[25] W.S. Opong, et al., Diffusive and convective protein transport through asymmetric membranes, AIChE J. 37 (10) (1991) 1497–1510, https://doi.org/10.1002/aic.690371007.
[26] Christl, I., et al., *Relating Ion Binding by Fulvic and Humic Acids to Chemical Composition and Molecular Size. 1. Proton Binding.* Environmental Science & Technology, 2001. **35**(12): p. 2505-2511. Doi: 10.1021/es0002518.
[27] K. Kimura, et al., Surface water biopolymer fractionation for fouling mitigation in low-pressure membranes, J. Membr. Sci. 554 (2018) 83–89, https://doi.org/10.1016/j.memsci.2018.02.024.
[28] N. Lee, et al., Low-pressure membrane (MF/UF) fouling associated with allochthonous versus autochthonous natural organic matter, Water Res. 40 (12) (2006) 2357–2368, https://doi.org/10.1016/j.watres.2006.04.023.
[29] R. Fabris, et al., Pre-treatments to reduce fouling of low pressure micro-filtration (MF) membranes, J. Membr. Sci. 289 (1) (2007) 231–240, https://doi.org/10.1016/j.memsci.2006.12.003.
[30] K. Tominaga, et al., Isolation of LC-OCD-quantified biopolymers from surface water: Significant differences between real biopolymers and model biopolymers, J. Membr. Sci. 658 (2022) 120714, https://doi.org/10.1016/j.memsci.2022.120714.
[31] T. Zhang, et al., Loose nanofiltration membranes for selective rejection of natural organic matter and mineral salts in drinking water treatment, J. Membr. Sci. 662 (2022) 120970, https://doi.org/10.1016/j.memsci.2022.120970.
[32] T. Bond, et al., Precursors of nitrogenous disinfection by-products in drinking water—A critical review and analysis, J. Hazard. Mater. 235–236 (2012) 1–16, https://doi.org/10.1016/j.jhazmat.2012.07.017.
[33] M. Yan, et al., Comparison of the effects of chloramine and chlorine on the aromaticity of dissolved organic matter and yields of disinfection by-products,

Chemosphere 191 (2018) 477–484, https://doi.org/10.1016/j.chemosphere.2017.10.063.
[34] J. Le Roux, et al., The role of aromatic precursors in the formation of haloacetamides by chloramination of dissolved organic matter, Water Res. 88 (2016) 371–379, https://doi.org/10.1016/j.watres.2015.10.036.
[35] A. Matilainen, et al., Natural organic matter removal by coagulation during drinking water treatment: A review, Adv. Colloid Interface Sci. 159 (2) (2010) 189–197, https://doi.org/10.1016/j.cis.2010.06.007.